Biophotonics Congress: Biomedical Optics Congress 2018 (Microscopy/Translational/Brain/OTS) © OSA 2018

A Tool for Quantitative and Systematic Simulation of Diffuse Optical Tomography with a Limited Number of Fixed Sources and Detectors

Edoardo Ferocino[1*], Antonio Pifferi[1,2], Simon Arridge[3], Fabrizio Martelli[4], Paola Taroni[1,2], Andrea Farina[2]
[1]*Politecnico di Milano, Dipartimento di Fisica, Piazza Leonardo da Vinci, 32, 20133, Milan, Italy*
[2]*Consiglio Nazionale delle Ricerche, Istituto di Fotonica e Nanotecnologie, Politecnico di Milano, Piazza Leonardo da Vinci, 32, 20133, Milan, Italy*
[3]*University College London, Department of Computer Science, Gower Street, London WC1E 6BT, United Kingdom*
[4]*Università degli Studi di Firenze, Dipartimento di Fisica e Astronomia, Via G. Sansone 1, 50019 Sesto Fiorentino, Firenze, Italy*
Email: edoardo.ferocino@polimi.it

Abstract: Quantitative Time-Domain Diffuse Optical Tomography simulations are systematically performed through a developed tool. Reflectance geometry and fixed sources and detectors provide 4 mm localization error and 80% accuracy on reconstructed absorption in depth (2 cm).
OCIS codes: (170.6960) Tomography; (170.6920) Time-resolved imaging; (110.0113) Imaging through turbid media

1. Introduction

In the field of medical imaging, tomography is an important tool for cancer detection and characterization e.g. for breast cancer and brain activation monitoring. When diffuse optical measurements are performed, exploiting the different combinations of sources and detectors arranged in a specific geometry, light probes a volume of the tissue, and a full 3D distribution of optical properties can be obtained, which correlates with the nature of the lesion. This technique is known as Diffuse Optical Tomography (DOT). An interesting approach to DOT, based on pulsed light sources, is called Time-Domain DOT (TD-DOT). This approach exploits the direct connection between time of flight (TOF) of detected photons (timing) and probed space. When working in reflectance geometry, the photon TOF encodes the photons penetration depth. Thus, TD DOT could be a valuable tool for in-depth breast cancer lesion characterization as can be built a hand-held probe with a limited number of sources and detection fibers for quick and non-invasive examinations. Still, to be used for lesion discrimination, TD DOT must provide a quantitative estimate of tissue composition to identify tissue type and lesion-related (or therapy-related) variations.

We here present the results of a series of systematic TD DOT simulations in reflectance geometry of a compact probe with a limited number of sources and detectors in a fixed geometry with the specific aim of assessing the capabilities on optical estimation and tissue composition quantification. The simulations are based on the analytical perturbation approach to the diffusion equation and consider realistic estimates of signal level and noise.

2. Methods

The TD DOT simulation is made up of two stages. The first, i.e. the forward problem, is the modeling of light propagation in a diffusive medium using the time-domain diffusion equation. The forward model, was first calculated for a homogeneous semi-infinite medium with fixed optical properties of background μ_a = 0.1 cm^{-1} and μ_s' = 10 cm^{-1} mimicking a healthy tissue. An absorbing spherical inclusion, mimicking the local alteration of optical properties (μ_a^{peak} = 0.2 cm^{-1}) of a tumor respect to the normal tissue, was placed at different positions underneath the surface. The inclusion was described by a Gaussian profile (σ = 0.5 cm). As the inclusion represents a small perturbation, considering both its volume and optical properties with respect to the background, we used the perturbative approach, under the Born approximation, to the diffusion equation [1].

The second stage was solving the inverse problem by finding the solution to the problem:

$$\min_{\Delta\mu_a}\left\{\left\|\frac{\Delta y - J\Delta\mu_a}{\sqrt{y_{hete}}}\right\|_2 + \tau\sigma_1(J)\|\Delta\mu_a\|_2\right\}$$

where $\Delta\mu_a$is the vector of the perturbed absorption for every voxel in rectangular mesh (6.4 x 5.8 x 3.2 cm^3, with 0.2 cm^3 voxel size), Δy is the difference between the time-resolved measurements obtained in the case with and without the inclusion, J is the Jacobian matrix calculated on 10 time windows ranging from 200 ps before to 3000 ps after the Instrument Response Function (IRF) peak/baricenter, $\sigma_1(J)$ is the maximum singular value of J, y_{hete} is the time-resolved measurement with perturbation and τ is a regularization parameter weighting the zero-order Tikhonov regularizer [2]. A rectangular pattern (x = 3 cm, y = 2 cm) was used to set both sources and detectors. On each long side, we arranged 4 pairs made of 1 source and 1 detector put at close distance (virtually null distance). The couples

were separated by 1 cm each. The measurement pattern exploited all the possible combinations of launching source and collecting detector at once, except for the combination including the source and the detector from the same spot (null-distance). The sources were defined by a typical IRF with a time-jitter (FWHM) of 230 ps. Poisson random noise was then added to the simulated data after a 1% Gaussian noise. To mimic a realistic situation, the effective photon number available at the detector was calculated considering a typical system responsivity, emitting power (1 mW @ 800 nm) and maximum count-rate (10^6 counts/s) for all the source-detector pairs. An hardware gating of the detector, capable to enhance the contribution of late-arriving photons, will be included in the simulations [3].

The DOT reconstruction quality was assessed by two main figures of merit:

i) the error on localization of the reconstructed inclusion along the three axes x, y and z with respect to the simulated position according to the center of mass

ii) the volumetric error on μ_a calculated as:

$$\epsilon_{vol} = \frac{\int_{ROI} \Delta\mu_a^{true} dV - \int_{ROI} \Delta\mu_a^{rec} dV}{\int_{ROI} \Delta\mu_a^{true} dV}$$

where ROI is a spherical region of interest (ROI) of radius 2 cm centered on the center of mass of the reconstructed inclusion and $\Delta\mu_a^{true}$ and $\Delta\mu_a^{rec}$ are the true and reconstructed absorption perturbation. A 3D Gaussian fit is performed to retrieve the volume of the reconstructed absorption distribution.

Other quantification parameters are provided such as the signal contrast, the contrast to noise ratio and indicators of the spatial distortion of the reconstructed sphere. A software tool for performing systematic simulations and quantification analysis was developed and employed to investigate automatically up to 5 simulation parameters at once, corresponding to around 5000 independent DOT reconstructions.

3. Results

As an example of a typical DOT reconstruction, Fig. 1 shows the 3D maps of an absorption heterogeneity set at a depth z = 1.5 cm. Fig. 1 left shows the simulated inclusion put in x = 1 cm, y = 0.5 cm position. On the right side, the reconstructed spherical inclusion is shown. A good localization is reached in x and y as the center of mass of the reconstructed inclusion is in x = 1 cm, y = 0.4 cm). Still is observed a broadening of the inclusion along the x-y axis respect to the original dimension and a flattening along the z dimension. At the same time, the inclusion is reconstructed at a smaller depth respect to the simulated. On the top layers, i.e. up to 7 mm can be seen artefacts caused by the presence of the surface.

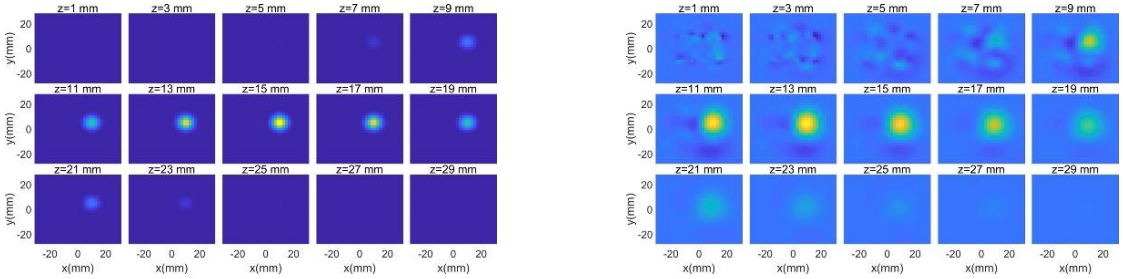

Fig. 1: Left: slices of a 6.4x5.8x3 cm3 volume where the simulated inclusion is a yellow spot. Right: the reconstructed inclusion with τ = 0.01.

The simulations can be repeated by placing the spherical perturbation in every point of the volume to assess the ability of the chosen configuration of sources and detectors in giving a good reconstruction in terms of localization, especially regarding the z-axis as can be directly related to the maximum depth that can be investigated in the tissue.

The systematic analysis for the localization error in z is displayed in Fig. 2. Each panel of Fig. 2 is a contour plot showing the error on the reconstructed z coordinate of the inclusion with respect to the true one (localization along the z-axis) expressed in millimeters. X and y axis of the contour plots are the x and y location of the heterogeneity beneath the probe (from x = -20 mm to x = 20 mm, from y = -10 mm to y = 10 mm), rows show the depth (from z = 5 mm to z = 20 mm) and columns the regularization parameter τ.The thick black line represents the error free region, while blue color indicates a negative error and red a positive one. The optimal region is identified by the green color. The effect of a growing regularization parameter is the smoothing of the error in the volume and reduction in the noise. Though with growing τ there is also an underestimation of the reconstructed z value, thus an increasing of the error for a fixed depth. For τ = 0.01, at the center of the rectangular pattern, there is a wide area of reduced error (maximum value is 4 mm) reaching 2 cm depth.

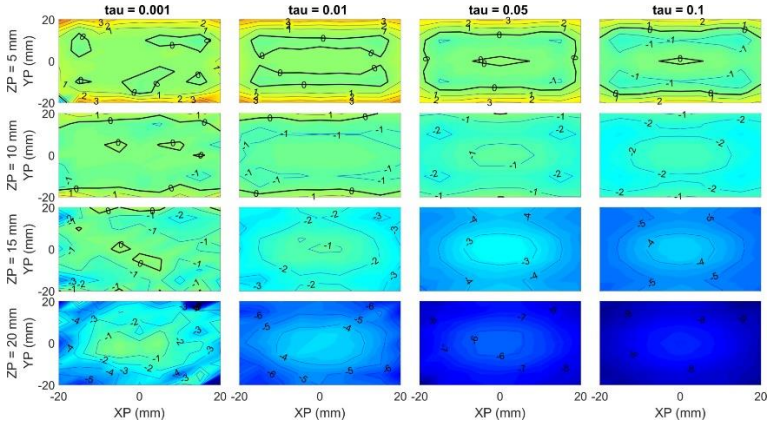

Fig. 2. Error on the localization of the inclusion along the Z-axis

Localization alone is not enough to guarantee a good lesion discrimination: the error on the reconstructed absorption coefficient must be considered. Fig. 3 shows the relative error over the quantification of the reconstructed absorption coefficient weighted for the reconstructed volume of the inclusion with respect to the simulated values, as discussed above. The errors are expressed as percentage. Can be still noticed the effect of a growing regularization that worsen the absorption estimate in favor of a smoother error distribution. At the same time, it is noticed the presence of a wide area up to 2 cm were the relative error is kept as low as 20%.

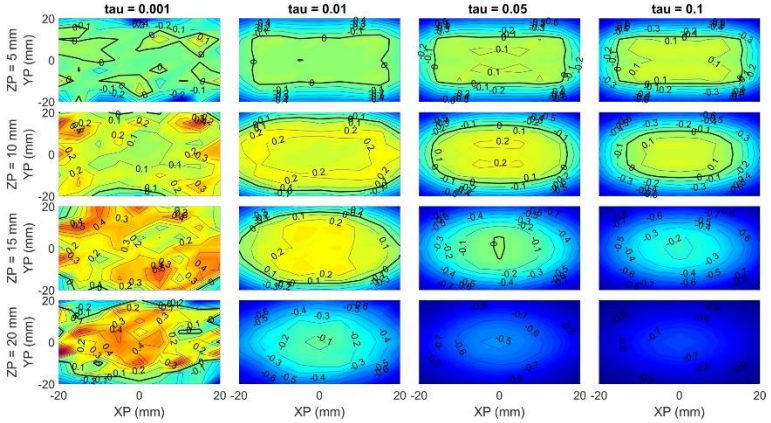

Fig. 3. Volumetric error on μ_a as described above

4. Conclusions

We developed a tool for systematic simulations for TD DOT on breast tissue, in reflectance geometry using a limited number of sources and detectors arranged in a rectangular pattern. The tool provides different figures of merit assessing the performance on lesion localization and reconstructed optical properties quantification.

The results have shown that the fixed configuration of sources and detectors efficiently localizes the inclusion, without the need for scanning movements, with localization errors lower that 4 mm and quantify the absorption coefficient with more than the 80% accuracy in a wide region under the sources and detectors up to 2 cm depth.

5. Acknowledgement

The research leading to these results has received partial funding from the European Union's Horizon 2020 research and innovation program under project SOLUS: "Smart Optical Laser and Ultrasound Diagnostics of Breast Cancer" (www.solus-project.eu, grant agreement No 731877). The project is an initiative of the Photonics Public Private Partnership. The authors declare that there are no conflicts of interest related to this article.

6. References

[1] F. Martelli, S. Del Bianco, A. Ismaelli, and G. Zaccanti, Light Propagation through Biological Tissue Light Propagation through Biological Tissue and Other Diffusive Media (SPIE Press Monograph, 2009).

[2] S. R. Arridge, "Optical tomography in medical imaging," Inverse Probl. **15**, R41–R93 (1999).

[3] A. Pifferi, A. Torricelli, L. Spinelli, D. Contini, R. Cubeddu, F. Martelli, G. Zaccanti, A. Tosi, A. Dalla Mora, F. Zappa, and S. Cova, "Time-resolved diffuse reflectance using small source-detector separation and fast single-photon gating," Phys. Rev. Lett. **100**, 1–4 (2008).